

## SIMULTANEOUS OBSERVATION OF RADAR AURORA AND VISIBLE AURORA OVER MIZUHO STATION

Tadahiko OGAWA<sup>1</sup>, Hisao YAMAGISHI<sup>2</sup>, Ichiro AYUKAWA<sup>2\*</sup>,  
Takashi TANAKA<sup>1</sup> and Kiyoshi IGARASHI<sup>1</sup>

<sup>1</sup>*Communications Research Laboratory, 2-1, Nukui-Kitamachi 4-chome, Koganei 184*

<sup>2</sup>*National Institute of Polar Research, 9-10, Kaga 1-chome, Itabashi-ku, Tokyo 173*

**Abstract:** Simultaneous observation of radar aurora and visible aurora in a small area ( $15 \times 20$  km) around an altitude of 100 km over Mizuho Station was made during a moderate substorm occurred before the midnight of October 5, 1985. The radar aurora was observed by a 50 MHz Doppler radar at Syowa Station while the visible aurora was monitored by a zenith photometer (4278 Å) with a view angle of about  $7^\circ$  at Mizuho Station, 270 km south-east of Syowa. It is found that within the bright auroral arc the radar echo intensity (therefore, the ionospheric electric field) is suppressed. Strong echoes caused by the gradient-drift instability appeared between the arcs. Within the faint, diffuse-like aurora which followed the bright arcs, the radar echoes due to the two-stream plasma instability driven by the electric field exceeding 25 mV/m were detected.

### 1. Introduction

The generation process of radar (radio) aurora is completely different from that of visible aurora. Radar aurora is caused by the electron density irregularities in the *E*-region due to plasma instabilities such as the gradient-drift and/or two-stream instabilities driven by electric field and/or electron density gradient (*e.g.*, OGAWA and IGARASHI, 1982). On the other hand, visible aurora in the *E*-region is produced by the energetic electrons of a few to 10 keV coming from the magnetosphere. Therefore, a simultaneous observation of radar and visible auroras in a common volume is important for understanding the electrodynamic environment of aurora.

Studies of the spatial relationship between radar and visible auroras began in the middle of 1950's (LYON, 1960). With advent of sophisticated radar, it has become clear that auroral arc appearing around midnight is not always collocated with radar aurora (BALSLEY *et al.*, 1973; GREENWALD *et al.*, 1973; TSUNODA *et al.*, 1976). Similar results have also been obtained at Syowa Station by IGARASHI and TSUZURAHARA (1981) and OGAWA and IGARASHI (1982). An anti-correlation between radar echo intensity and auroral arc luminosity is believed to be caused by the suppression of electric field due to a high electron density within the arc (DE LA BEAUJARDIERE *et al.*, 1977), thereby also suppressing the plasma instabilities which depend on electric field strength.

In the auroral radar experiments made by BALSLEY *et al.* (1973), GREENWALD

---

\* Now at Fujitsu Limited.

*et al.* (1973) and TSUNODA *et al.* (1976), the spatial resolutions of the radar in a horizontal plane were less than  $25 \times 45$  km. For a comparison of radar echo region and auroral luminosity, they used all-sky photographs which do not always provide a sufficient spatial resolution. Using an auroral radar at Syowa Station ( $69^{\circ}00'S$ ,  $39^{\circ}35'E$ ; geomagnetic coordinates,  $70.0^{\circ}S$ ,  $79.4^{\circ}E$ ) and a zenith photometer at Mizuho Station ( $70^{\circ}42'S$ ,  $44^{\circ}20'E$ ; geomagnetic coordinates,  $72.3^{\circ}S$ ,  $80.6^{\circ}E$ ), 270 km south-east of Syowa, IGARASHI and TSUZURAHARA (1981) have examined the correlation between radar echo intensity and visible aurora luminosity over Mizuho. In this case, the radar beamwidth in azimuth was very wide (about  $30^{\circ}$ ) while the view angle of photometer was about  $5^{\circ}$ , and therefore the area ( $100 \times 200$  km) viewed by the radar was extremely wider than that by the photometer. OGAWA and IGARASHI (1982) have utilized the same radar together with a scanning-photometer at Syowa Station and discussed the relation among auroral form, echo power and Doppler spectrum. None of the experiments described above, however, seems satisfactory for clarifying the detailed spatial and temporal relationships between radar aurora and visible aurora.

A new 50 MHz auroral Doppler radar with a narrow azimuthal beamwidth of about  $4^{\circ}$  was set up at Syowa Station in 1982 (IGARASHI *et al.*, 1982). During the period from August to October 1985, this radar measured the echo power and Doppler spectrum over Mizuho Station where a 4278 A photometer looking the zenith with a view angle of about  $7^{\circ}$  was installed. This setup enables us to explore the auroral phenomena in a common viewing area of about  $15 \times 20$  km. As a case study, this paper reports the results obtained during the substorm event before midnight of October 5, 1985.

## 2. Experiment

Figure 1 illustrates an experimental configuration in the magnetic meridian and horizontal planes. The 50 MHz auroral Doppler radar at Syowa Station has two radar beams with a crossing angle of about  $33^{\circ}$  (IGARASHI *et al.*, 1982); one toward magnetic south (GMS beam,  $133.7^{\circ}$  azimuth from north to east), that is, just toward Mizuho Station, and the other toward approximately geographic south (GGS beam,  $166.4^{\circ}$  azimuth). Each beam has a vertical beamwidth of about  $30^{\circ}$  and an azimuthal beamwidth of about  $4^{\circ}$ . The radar transmitted a pulse of  $100 \mu s$  length (range resolution of 15 km) with a pulse repetition frequency of 333 Hz (maximum unaliasing Doppler velocity of  $\pm 500$  m/s). Therefore the spatial resolution in the horizontal plane becomes about  $15 \times 20$  km at the slant range of 285 km over Mizuho. The auroral radar echoes are known to return from the electrojet altitudes. By assuming a vertical thickness of the electrojet to be 10 km, the volume viewed by the radar is approximately  $15 \times 20 \times 10$  km.

The auroral luminosity was monitored at Mizuho by a zenith photometer of 4278 A with a view angle of about  $7^{\circ}$ . This yields the spatial resolution of 12 km at 100 km altitude under the assumption that 4278 A luminosity is most intense at about 100 km. Thus, the setup shown in Fig. 1 enables us to make a simultaneous observation of aurora in a small common volume by the radar and photometer.

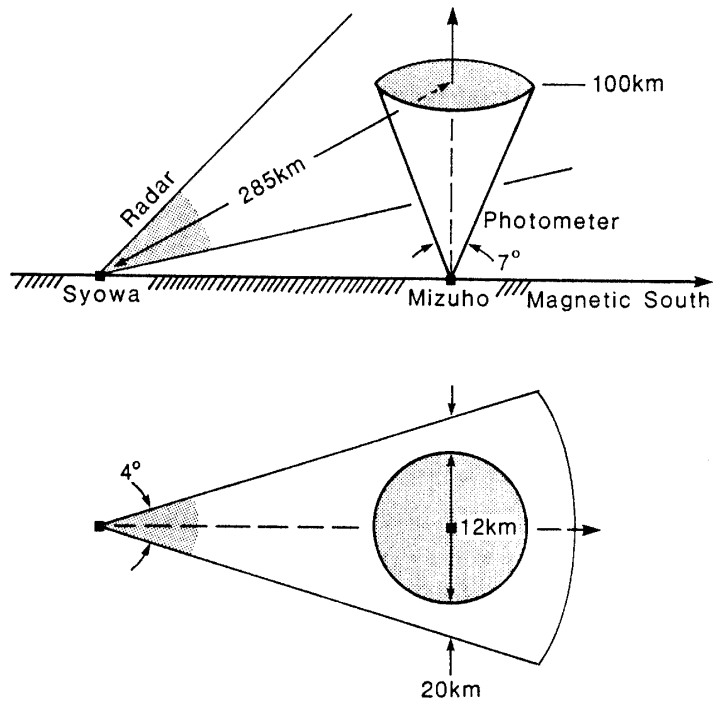


Fig. 1. Configuration of the experiment in magnetic meridian plane (upper) and horizontal plane (lower). Radar and photometer are located at Syowa and Mizuho, respectively.

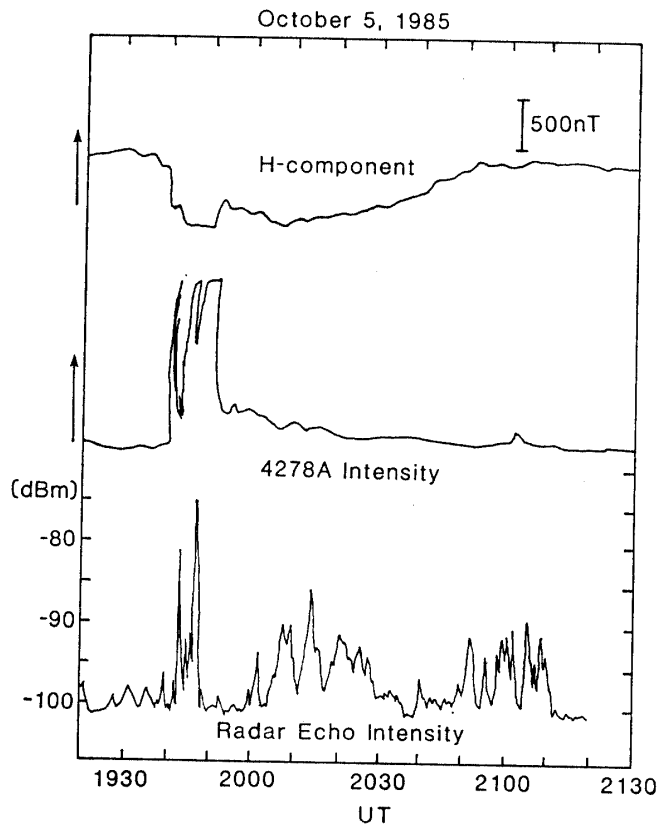


Fig. 2. Time variations of geomagnetic H-component at Mizuho (top), 4278 A auroral intensity over Mizuho (middle) and radar echo intensity at 285 km range on the GMS beam from Syowa on October 5, 1985. Note the saturation of auroral intensity around 1946 and 1950 UT.

### 3. Results

A moderate substorm occurred before the midnight of October 5, 1985. Figure 2 shows the time variations of the geomagnetic  $H$ -component at Mizuho, the 4278 A intensity over Mizuho and the radar echo intensity at the slant range of 285 km from Syowa Station. In association with a large depression of the  $H$ -component during 1940–1951 UT (UT=LT–3 hours), both the auroral intensity and the radar echo intensity increased. After 1951 UT, the auroral intensity due to faint, diffuse-like aurora remained at a low level while the echo intensity increased quite often. In order to see in more detail the relationship between the auroral and echo intensities during 1930–2000 UT, Fig. 2 is enlarged in Fig. 3 where the echo intensity is plotted every 26 s. It is very easy to observe a clear anti-correlation between them. The auroras between 1940 and 1951 UT can be regarded as the multiple auroral arcs which traversed successively the field-of-view of the Mizuho photometer.

Contour map of the radar echo intensity as a function of time and range obtained by the GMS beam is shown in Fig. 4. Since the echo intensity depends strongly on the aspect angle, which is defined by the angle between radar beam and geomagnetic field vectors, most of the echoes return from the ranges of 240–345 km corre-

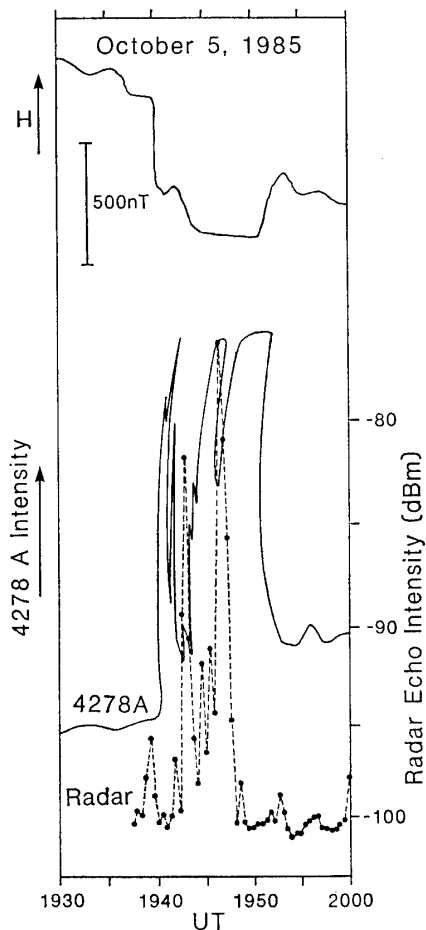


Fig. 3. Same as Fig. 2, but for the enlargement of Fig. 2 during 1930–2000 UT.

sponding to the aspect angles of  $85^{\circ}$ – $95^{\circ}$ . As can be seen in Fig. 4, the strong echo region moved from south to north during 1946–1947 UT with a velocity of about 1.3 km/s, which suggests that the multiple arcs also moved from south to north with the same velocity. Unfortunately, this movement was not confirmed by the Syowa all-sky photographs because of bad weather.

Figure 5 shows the Doppler velocity spectra, covering the time period of Fig. 2, obtained every 52 s at particular points on the GGS (range=345 km) and GMS (285 km) beams. These two points are located on the same  $L$ -value (7.3) with a separation of about 240 km. The plus (minus) sign means that the velocity is toward (away from) Syowa Station. From the Doppler spectra and the geometrical configuration of the GGS and GMS radar beams described in section 2, the following two facts can be pointed out. First, the electric fields causing the plasma instabilities

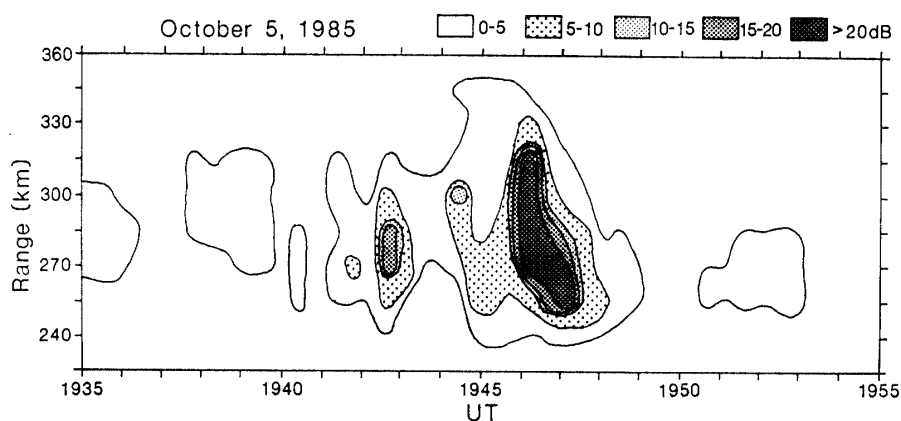


Fig. 4. Contour map (range-time intensity display) of radar echo intensity with 5 dB spacing obtained by the GMS antenna beam.

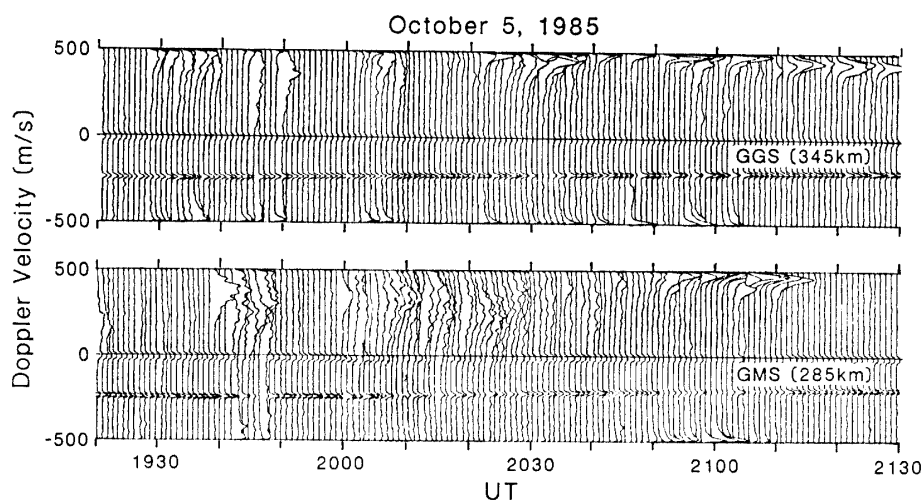


Fig. 5. Doppler velocity spectra at 345 km range on the GGS beam (upper) and 285 km range on the GMS beam (lower). One spectrum shown in the figure was obtained by 128-point FFT of echo signals for 384 ms and then by averaging successive 20 spectra over 7.68 s. Almost continuous curves appearing between  $-200$  and  $-250$  m/s are due to receiver noise interference and should be neglected.

(irregularities) intruded from the west toward Mizuho, since there exists a time delay of about 10 minutes between the onsets of the GGS (1928 UT) and GMS (1938 UT) echoes. Second, the electric fields associated with the arcs during 1938–1948 UT had westward components with strengths less than, say 20 mV/m, since the spectral peaks corresponding to the  $\mathbf{E} \times \mathbf{B}$  drifts appear at plus Doppler velocities which are less than 400 m/s. The irregularities causing these echoes are driven by the gradient-drift instability as will be discussed later. Judging from the  $H$ -component variation in Fig. 2, the westward electrojets due to the northward electric fields were flowing in association with the arcs. By combining the  $H$ -component and Doppler velocity measurements, it may be concluded that the electric fields around the auroral arcs were directed north-westward.

In Fig. 2, the radar echo intensity became quite often strong after 2000 UT when the auroral intensity was very low. The Doppler spectra on the GMS beam in Fig. 5 indicate that the irregularities are due to the gradient-drift instability during 2000–2040 UT and to the two-stream instability driven by the electric fields exceeding 25 mV/m (Doppler velocity of 500 m/s) during 2050–2110 UT. The two-stream spectra also appear on the GGS beam during the latter period, suggesting that the strong electric fields prevailed over a wide area.

#### 4. Discussion and Summary

Based on Figs. 3, 4 and 5 and the results presented in section 3, we discuss the spatial relationship between the auroral arcs and the irregularities (electric fields). Here we simply assume that the temporal variations shown in Fig. 3 can be regarded as the spatial variations. Figure 6 illustrates very schematically the arc system and the irregularity regions in the magnetic meridian plane. The irregularities and perhaps the arcs moved from south to north (see Fig. 4). This movement can be related to the magnetospheric plasma convection associated with the substorm. The stronger

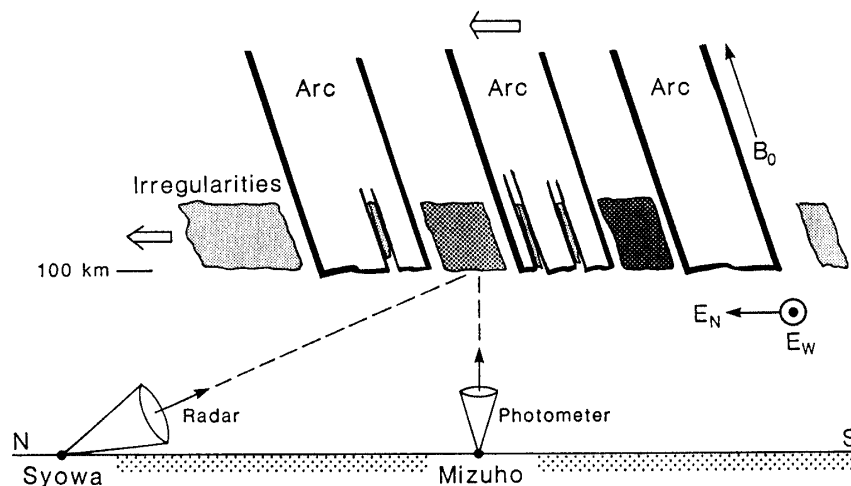


Fig. 6. Schematic illustration of the spatial relationship between auroral arcs and irregularity regions causing radar echoes. The darker shaded part represents the stronger echo region. See text for detail.

irregularities are located between the neighboring arcs, while weaker ones appear on both the equator and pole sides of the arc system and also in the faint luminosity regions in each arc (see Fig. 3). The irregularities were driven by the gradient-drift instability (see Fig. 5) which occurred under the combined action of the electron density gradient and the electric field parallel to the density gradient. Since the auroral arc is necessarily accompanied by the horizontal gradients, no occurrence of irregularities within the arc means the absence of strong electric field. The electric field within the arc may be reduced by a southward arc-associated polarization field, resulting in the suppression of the plasma instability. Outside the arcs, the north-westward electric fields of the order of 20 mV/m are inferred from the Doppler spectra in Fig. 5.

In summary, a case study of the simultaneous observation of the radar aurora and the visible aurora in a small area has been reported. It is found that within the bright auroral arc the radar echo intensity (electric field) is suppressed. This finding supports the previous results by other investigators. An interesting fact is that the strong radar echoes due to the gradient-drift plasma instability appeared between the arcs. This relationship has not been clear so far. Within the faint, diffuse-like aurora which followed the bright arcs, the radar echoes due to the two-stream instability driven by the electric field exceeding 25 mV/m were detected. Such strong fields associated with the faint aurora were also observed by OGAWA and IGARASHI (1982).

#### Acknowledgments

We would like to thank the staff of the National Institute of Polar Research and the wintering members of the 26th Japanese Antarctic Research Expedition (1985–1986) for their kind support to our experiment.

#### References

- BALSLEY, B. B., ECKLUND, W. L. and GREENWALD, R. A. (1973): VHF Doppler spectra of radar echoes associated with a visual form; Observations and implications. *J. Geophys. Res.*, **78**, 1681–1687.
- DE LA BEAUJARDIERE, O., VONDRAK, R. and BARON, M. (1977): Radar observations of electric fields and currents associated with auroral arcs. *J. Geophys. Res.*, **82**, 5051–5062.
- GREENWALD, R. A., ECKLUND, W. L. and BALSLEY, B. B. (1973): Auroral currents, irregularities and luminosity. *J. Geophys. Res.*, **78**, 8193–8203.
- IGARASHI, K. and TSUZURAHARA, S. (1981): Spatial correlations between radio aurora and 4278 A aurora intensity. *Mem. Natl Inst. Polar Res., Spec. Issue*, **18**, 204–211.
- IGARASHI, K., OGAWA, T., OSE, M., FUJII, R. and HIRASAWA, T. (1982): A new VHF Doppler radar experiment at Syowa Station, Antarctica. *Mem. Natl Inst. Polar Res., Spec. Issue*, **22**, 258–267.
- LYON, G. F. (1960): The association of visible auroral forms with radar echoes. *Can. J. Phys.*, **38**, 385–389.
- OGAWA, T. and IGARASHI, K. (1982): VHF radar observation of auroral *E*-region irregularities associated with moving-arcs. *Mem. Natl Inst. Polar Res., Spec. Issue*, **22**, 125–139.
- TSUNODA, R. T., PRESNELL, R. I., KAMIDE, Y. and AKASOFU, S.-I. (1976): Relationship of radar aurora, visual aurora, and auroral electrojets in the evening sector. *J. Geophys. Res.*, **81**, 6005–6015.

(Received September 8, 1988; Revised manuscript received January 9, 1989)